

Appendix A: Supplementary data

A simple and generic post-treatment strategy for highly efficient Cr³⁺- activated broadband NIR emitting phosphors for high-power NIR light sources

Zhi-hang Zheng, ^a *Bo-Mei Liu* ^{a*}, *Zhi Zhou* ^b, Chong-Geng Ma,^c and Jing Wang^{a*}

^a Ministry of Education Key Laboratory of Bioinorganic and Synthetic Chemistry
State Key Laboratory of Optoelectronic Materials and Technologies
School of Chemistry, School of Materials Science and Engineering
Sun Yat-Sen University, Guangzhou 510275, China

^b Prof. Z. Zhou
College of Science
Hunan Optical Agriculture Engineering Technology Research Center
Hunan Agricultural University, Changsha City, Hunan 10128, China

^c CQUPT-BUL Innovation Institute, Chongqing University of Posts and
Telecommunications, No. 2 Chongwen Road, Nan'an District, Chongqing 400065,
China

* Corresponding authors.

E-mail address: liubm6@mail.sysu.edu.cn (B-M Liu), ceswj@mail.sysu.edu.cn (J. Wang)

Synthetic procedures of LiScO₂:Cr³⁺

LiScO₂:0.03Cr³⁺ phosphors were synthesized by high-temperature solid-state reaction. Li₂CO₃ (99.8%), Sc₂O₃ (99.99%), and Cr₂O₃ (99.99%) were used as starting materials and weighed in stoichiometric proportions, except that 5% excess of Li₂CO₃ was used to compensate its evaporation loss during a high-temperature reaction. The powder mixture was ground thoroughly in an agate mortar and then transferred into an alumina crucible, followed by sintering at 1150°C for 2h in air.

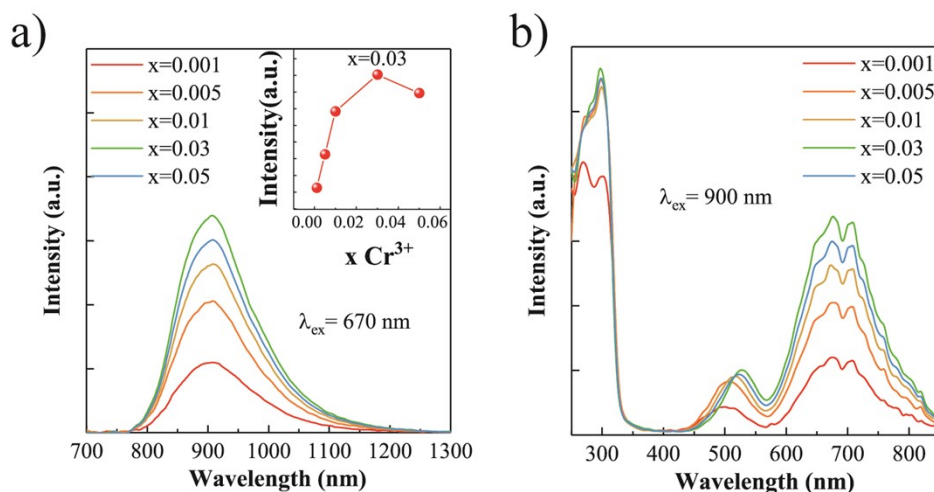


Figure S1. (a) Emission and (b) excitation spectra of $\text{LiInO}_2:\text{xCr}^{3+}$ ($x=0.001$ - 0.05) phosphors. Inset: concentration dependence of relative emission intensity.

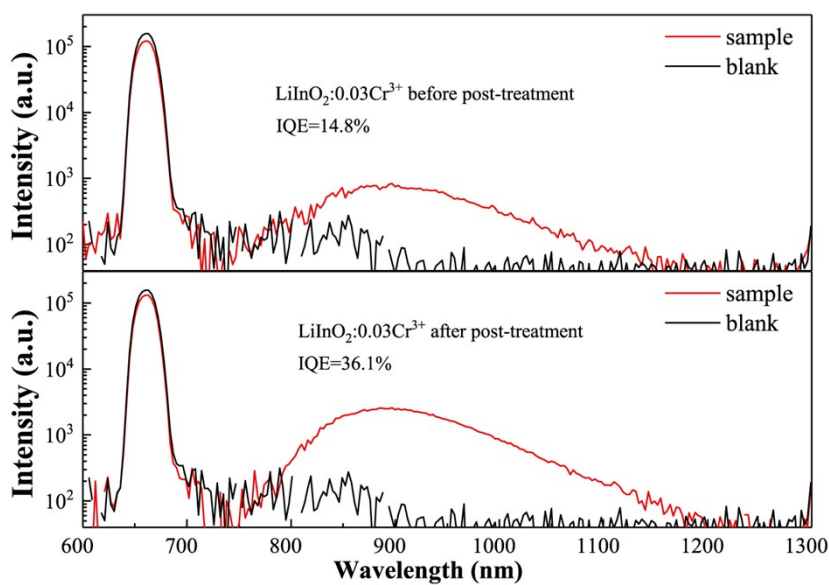


Figure S2. The IQE of $\text{LiInO}_2:0.03\text{Cr}^{3+}$ before and after post-treatment. The IQE of $\text{LiInO}_2:0.03\text{Cr}^{3+}$ increased from 14.8% to 36.1% after post-treatment.

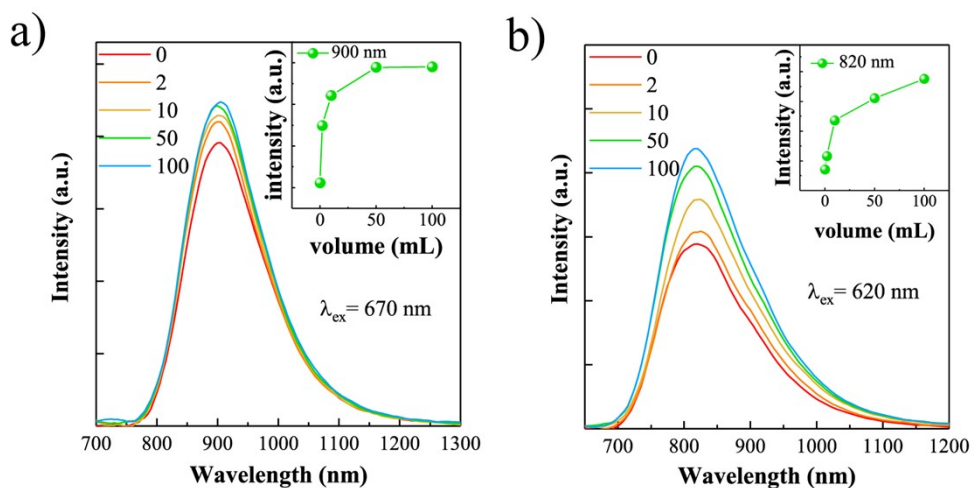


Figure S3. (a) PL of $\text{LiInO}_2:0.03\text{Cr}^{3+}$ and (b) $\text{LiScO}_2:0.03\text{Cr}^{3+}$ with different water volume (0-100 mL). With the increase of the water volume, the emission intensity at 900 nm and 820 nm rise and eventually stabilize.

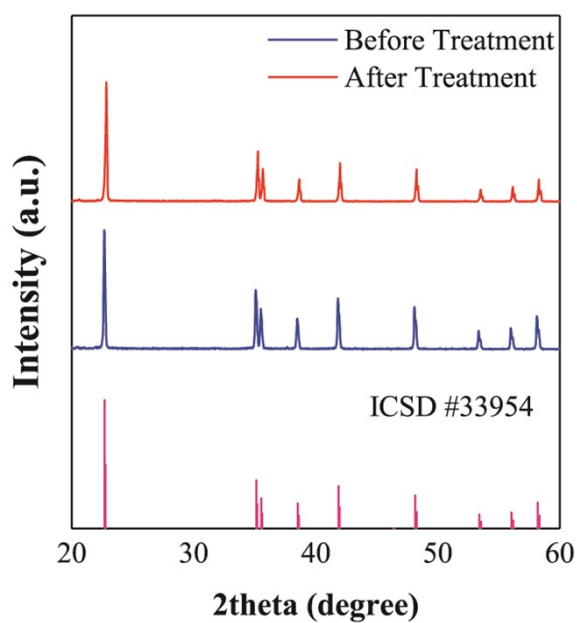


Figure S4. The XRD pattern of $\text{LiInO}_2:0.03\text{Cr}^{3+}$ before and after post-treatment.

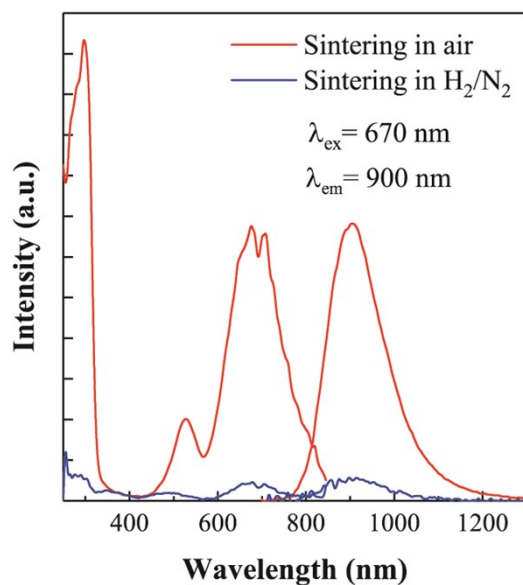


Figure S5. PL and PLE spectra of $\text{LiInO}_2:0.03\text{Cr}^{3+}$ sintering in air and in H_2/N_2 atmosphere at 1000°C for 2h. We can find that after sintering in H_2/N_2 atmosphere, the $\text{LiInO}_2:0.03\text{Cr}^{3+}$ phosphor shows poor luminescence properties comparing with the sample sintering in air.

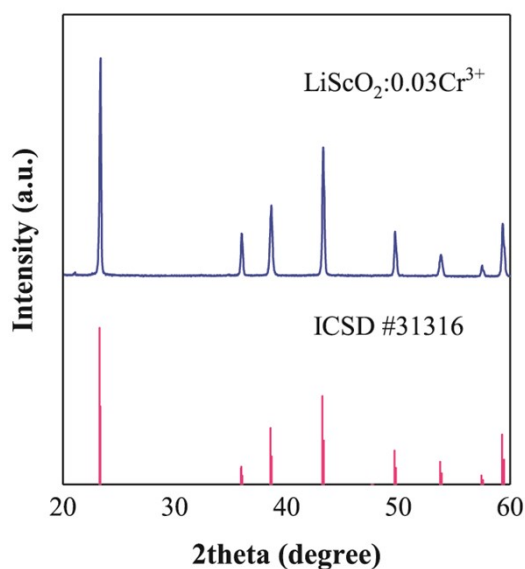


Figure S6. The XRD pattern of $\text{LiScO}_2:0.03\text{Cr}^{3+}$. Compared to the reference spectrum of LiScO_2 (ICSD #31316), no impurities occur when the doping ratio of Cr^{3+} is 0.03, LiScO_2 crystals were successfully prepared by high-temperature solid-state method.

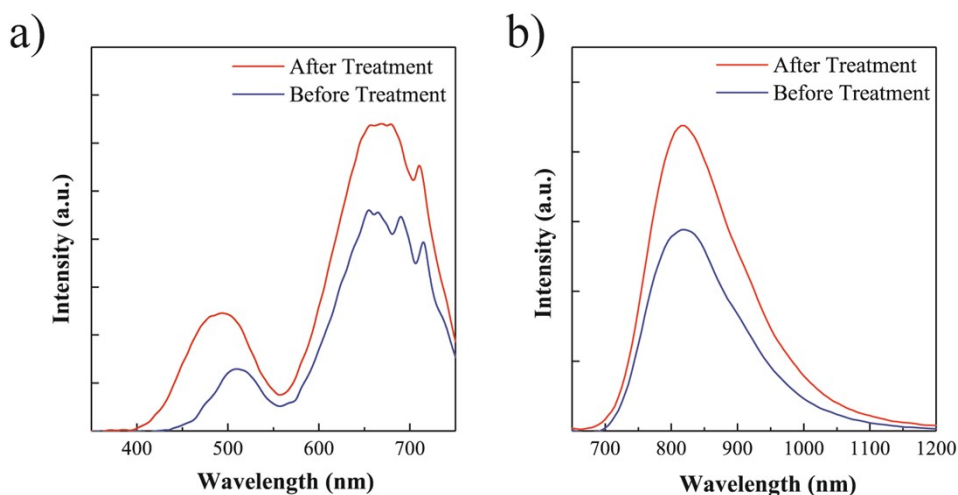


Figure S7. (a)(b) PL and PLE spectra of $\text{LiScO}_2:0.03\text{Cr}^{3+}$ after post-treatment. The intensity of $\text{LiScO}_2:0.03\text{Cr}^{3+}$ in 820 nm enhanced 41.8% after post-treatment.

Host	EQE (%)		Increment	Treating liquid	Ref.
	After Treatment	Before Treatment			
LiScGeO_4	4.1%	2.8%	1.3%	A*	1
$\text{LiInGe}_2\text{O}_6$	37.8%	27.1%	10.7%	A*	2
$\text{LiIn}_2\text{SbO}_6$	6.3%	5.2%	1.1%	A*	3
$\text{NaInGe}_2\text{O}_6$	17.1%	15.4%	1.7%	A*	4
$\text{LiInSi}_2\text{O}_6$	34.4%	31.7%	2.7%	A*	5
LiGa_5O_8	30.5%	25.4%	5.1%	A*	6
$\text{Ca}_3\text{Sc}_2\text{Si}_3\text{O}_{12}$	2.9%	1.6%	1.3%	A*	7
$\text{Gd}_3\text{Sc}_2\text{Ga}_3\text{O}_{12}$	14.6%	11.5%	3.1%	A*	8
LiInO_2	11.9%	3.3%	8.6%	W*	This work
LiScO_2	13.4%	8.1%	5.3%	W*	This work

Figure S8. Results of the EQE of the Cr^{3+} -activated phosphors before and after post-treatment. A* = diluted nitric acid; W* = deionized water

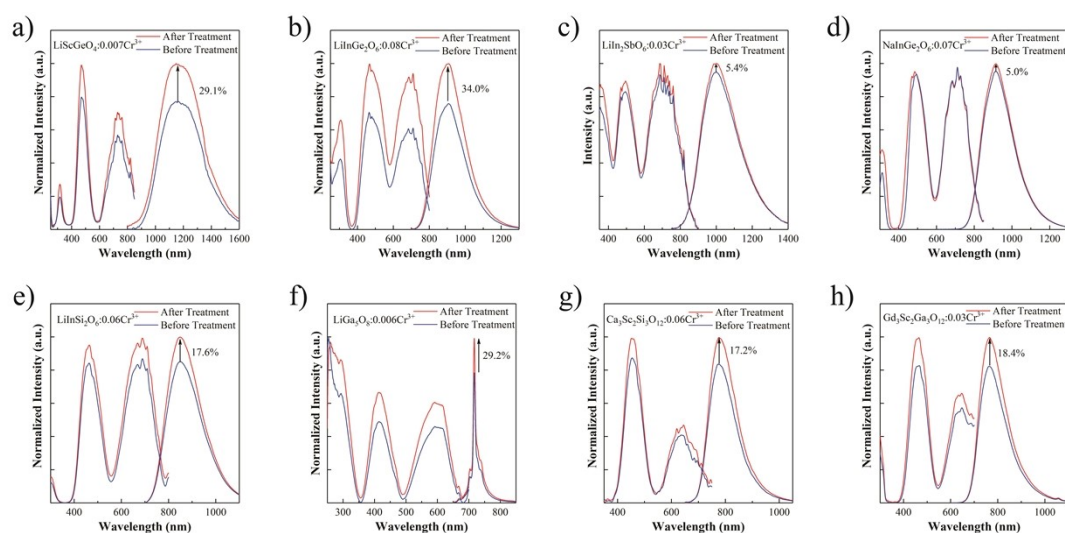


Figure S9. (a) ~ (h) PL and PLE spectra of the reported Cr^{3+} -doped NIR phosphors before and after post-treatment. It can be found that after post-treatment, the NIR emission of the phosphors enhanced. (a) $\text{LiScGeO}_4:0.007\text{Cr}^{3+}$, (b) $\text{LiInGe}_2\text{O}_6:0.08\text{Cr}^{3+}$, (c) $\text{LiIn}_2\text{SbO}_6:0.03\text{Cr}^{3+}$, (d) $\text{NaInGe}_2\text{O}_6:0.07\text{Cr}^{3+}$, (e) $\text{LiInSi}_2\text{O}_6:0.06\text{Cr}^{3+}$, (f) $\text{LiGa}_5\text{O}_8:0.006\text{Cr}^{3+}$, (g) $\text{Ca}_3\text{Sc}_2\text{Si}_3\text{O}_{12}:0.06\text{Cr}^{3+}$, (h) $\text{Gd}_3\text{Sc}_2\text{Ga}_3\text{O}_{12}:0.03\text{Cr}^{3+}$

Table S1. Results of the ICP-AES of the $\text{LiInO}_2:0.03\text{Cr}^{3+}$ phosphor before and after post-treatment.

Sample	Concentration of Cr/ $\text{mg}\cdot\text{kg}^{-1}$	Weight of Cr/mg
$\text{LiInO}_2:0.03\text{Cr}^{3+}$ precursor	8469.0	4.23
supernatant after treatment	7.01	3.50

References

1. Z. Ye, Z. Wang, Q. Wu, X. Huo, H. Yang, Y. Wang, D. Wang, J. Zhao, H. Suo and P. Li, *Dalton Trans*, 2021, **50**, 10092-10101.
2. T. Liu, H. Cai, N. Mao, Z. Song and Q. Liu, *Journal of the American Ceramic Society*, 2021, **104**, 4577-4584.
3. G. Liu, T. Hu, M. S. Molokeev and Z. Xia, *iScience*, 2021, **24**, 102250.
4. W. Zhou, J. Luo, J. Fan, H. Pan, S. Zeng, L. Zhou, Q. Pang and X. Zhang, *Ceramics International*, 2021, **47**, 25343-25349.
5. X. Xu, Q. Shao, L. Yao, Y. Dong and J. Jiang, *Chemical Engineering Journal*, 2020, **383**, 123108.
6. P. Xiong, B. Huang, D. Peng, B. Viana, M. Peng and Z. Ma, *Advanced Functional Materials*, 2021, **31**, 2010685.
7. Z. Jia, C. Yuan, Y. Liu, X. J. Wang, P. Sun, L. Wang, H. Jiang and J. Jiang, *Light Sci Appl*, 2020, **9**, 86.
8. E. T. Basore, W. Xiao, X. Liu, J. Wu and J. Qiu, *Advanced Optical Materials*, 2020, **8**, 2000296.